Classification: BIOLOGICAL SCIENCES / Plant Bilogy

Title:

MAB4-induced auxin sink generates local auxin gradients in *Arabidopsis* organ formation

Author affiliation:

Masahiko Furutani[1], Yasukazu Nakano[1], Masao Tasaka[1]

[1]Graduate School of Biological Sciences, Nara Institute of Science and Technology (NAIST), Takayama 8916-5, Ikoma, Nara 630-0192, Japan

Corresponding author:

Masahiko Furutani and Masao Tasaka

Takayama 8916-5, Nara 630-0192, Japan

To M.F.

+81-743-72-5485

ma-furut@bs.naist.jp

To M.T.

+81-743-72-5480

m-tasaka@bs.naist.jp

Keywords:

Organ formation, auxin transport, PIN polarity, NPH3-like proteins

Significance Statements

The dynamic auxin transport driven by the auxin efflux carrier PIN-FORMED1 (PIN1) is the key element in organ formation at the shoot apical meristem. Auxin transport during organ formation consists of two distinct types: the convergence of auxin flow at the organ initiation site and the following auxin sink. Our results show that NPH3-like proteins establish auxin sink, but not auxin convergence, through the control of PIN1 localization. Our study is the first to uncover the molecular mechanism involved in auxin sink and to show its importance in organ development. Besides, we propose a model for polar auxin transport during organ formation, which has the potential to describe on a molecular level the auxin canalization hypothesis proposed by Sachs (1981).

Abstract

In *Arabidopsis*, leaves and flowers form cyclically in the shoot meristem periphery and are triggered by local accumulations of the plant hormone auxin (1). Auxin maxima are established by the auxin efflux carrier PIN-FORMED1 (PIN1) (2, 3, 4). During organ formation, two distinct types of PIN1 polarization occur (5). First, convergence of PIN1 polarity in the surface of the meristem creates local auxin peaks. Second, basipetal PIN1 polarization causes auxin to move away from the surface in the middle of an incipient organ primordium, thought to contribute to vascular formation. Several mathematical models have been developed in attempts to explain the PIN1 localization pattern (6, 7, 8, 9). However, the molecular mechanisms that control these dynamic changes are unknown. Here we show that loss-of-function in the *MACCHI-BOU 4* (*MAB4*) family genes, which encode NON-PHOTOTROPIC HYPOCOTYL 3 (NPH3)-like proteins and regulate PIN endocytosis (10-13), causes deletion of basipetal PIN1 polarization, resulting in extensive auxin accumulation all over the meristem surface from lack of a sink for auxin. These results indicate that the *MAB4* family genes establish inward auxin transport from the L1 surface of incipient organ primordia by basipetal PIN1 polarization, and that this behavior is essential for the progression of organ development. Furthermore, the expression of the *MAB4* family genes depends on auxin response. Our results define two distinct molecular mechanisms for PIN1 polarization during organ development and indicate that an auxin response triggers the switching between these two mechanisms.

/body

Introduction

In *Arabidopsis*, organ primordia are initiated in a spiral manner in the periphery of the meristem. These primorida then form bulges and progressively develop into organs in a process controlled by the plant hormone auxin (1). Prior to the formation of primordia, local auxin accumulation is established by a polar auxin transport system that is predominantly driven by the polarized auxin efflux carrier PIN-FORMED1 (PIN1) (2, 3). During organ development, PIN1 polarity undergoes a dynamic change (4, 5). Initially, PIN1 polarity points to the center of the incipient organ primordium in the L1 surface layer of the meristem and induces the local accumulation of auxin. Then, PIN1 polarity changes when the organ primordium begins to grow; in the center of the organ primordium, PIN1 polarity becomes basipetal, leading to the establishment of an auxin sink. Several mathematical models have been developed in attempts to explain the PIN1 localization pattern (6-9). Although no simple model is sufficient to encompass all the dynamic behavior of PIN1 localization in the meristem, Bayer et al. recently proposed the integration of two of these models to explain convergent PIN1 polarity and basipetal PIN1 polarization (5). Several genes that play a key role in auxin-dependent organ development have been identified; however, the molecular mechanisms that might confirm the mathematical models have not yet to been identified. The *pinoid* (*pid*) and *monopteros* (*mp*) mutants display severe defects in organ formation leading to pin-shaped inflorescences; these phenotypes resemble those of *pin1* mutants (14-16). *PID* encodes a Ser/Thr kinase that controls PIN1 polarity through the direct phosphorylation of the PIN1 protein (17-19). Depletion of *PID* results in an apical-to-basal shift of PIN1 localization in the surface of the inflorescence meristem, indicating that *PID* controls apical-basal PIN1 polar targeting (20). *MP* encodes a transcription factor, AUXIN RESPONSE FACTOR 5 (ARF5), that mediates auxin

response during organ development (21). In addition, NON-PHOTOTROPIC HYPOCOTYL 3 (NPH3)-like proteins, including MACCHI-BOU 4 /ENHANCER OF PINOID/NAKED PINS IN YUC MUTANTS 1 (MAB4/ENP/NPY1), have been identified as key regulators of PIN localization during cotyledon development and in root gravitropism (10-13, 22). However, because their roles have been investigated only in the steady state, it is unclear how they act in a dynamic process, organ formation in the meristem. In this study, we investigated the function of *MAB4* family genes in organ formation at the shoot meristem. We show that *MAB4* family genes, after induction by an MP-mediated auxin response, promote organ development through the establishment of basipetal auxin flow, pointing out the importance of auxin sink during organ formation. Our findings prove the existence of two distinct molecular mechanisms for PIN1 polarization in organ development and suggest that differences in auxin responses permit these distinct mechanisms to coexist in the same developmental program.

Results and Discussion

MAB4 family genes establish inward auxin transport during flower development

The severity of the abnormal phenotype in *mab4* mutants is enhanced by mutations of other *MAB4* family member genes, *MAB4/ENP/NPY1-LIKE1* (*MEL1*)/*NPY3* and *MEL2*/*NPY5*, during flower development. *mab4*/*enp*/*npy1* single mutants display mild defects in organ formation including cotyledons and floral organs (10, 11, 22). The combination of *mab4* and *mel1*/*npy3* mutations resulted in the formation of pin-like inflorescences with several leaves and fertile flowers (Fig. S1*A*). In contrast, at a low frequency, *mab4 mel2/npy5* double mutants developed pin-like inflorescences with several leaves and sterile flowers (Fig. S1*B*). Subsequently, we constructed *mab4-2 mel1-1 mel2-1* triple mutants and these displayed a more severe pin-like inflorescence than *mab4-2 mel1-1* and *mab4-2 mel2-1* double mutants (Fig. 1*A* and *B*). These results were consistent with previous observation of multiple mutants between *npy1*, *npy3*, and *npy5* (12). This indicates that *MAB4* family genes control flower development redundantly at the inflorescence meristem. To further investigate the function of *MAB4* family genes, we compared expression of the auxin responsive marker *DR5rev::GFP* (23) and PIN1-GFP in the wild-type inflorescence meristem and the *mab4-2 mel1-1 mel2-1* triple mutant, which has a pin-shaped meristem. In the wild-type meristem, *DR5rev::GFP* expression was identified only in the L1 surface layer of the flower initiation site (Fig. 1*C*). As the organ primordium developed, the GFP signal was present not only in the L1 layer but also in the inner cell layers (Fig. 1*D* and *E*). Concomitantly, *DR5rev::GFP* expression in the L1 layer narrowed to a few cells (Fig. 1*F*). Corresponding with this change in expression pattern, the PIN1-GFP signal was detected in the epidermis and prospective vasculature of incipient and developing flower primordia. PIN1-GFP was localized to the side of the plasma membrane closer to

the center of incipient flower primordia (Fig. 1*G*); as the flower primordium bulge grew, the PIN1-GFP signal was found to be present in both the anticlinal side and the inner side of the epidermis and in the inner cells of the young organ primordium (Fig. 1*H* and *I,* Fig. S2). These results indicate that initially the concentration of auxin in the L1 surface layer of the incipient flower primordium is increased by an active pump mechanism (Fig. 1*G-I*; white arrows) and that subsequently basipetal auxin transport is gradually established from the L1 layer in the middle of the organ primordium (Fig. 1*H* and *I*; orange arrows). These findings suggest the presence of a two-step control of auxin flow in the wild-type meristem.

By contrast to the wild-type, *DR5rev::GFP* was present over all the epidermis of the peripheral region of the pin-shaped inflorescence meristem in the *mab4 mel1 mel2* triple mutants; however, the GFP signals showed non-uniform intensities (Fig. 1*J* and *K*). Interestingly, we could not detect any *DR5rev::GFP* signals in the inner cells of the mutant meristem. Consistent with these observations, PIN1-GFP localization was severely disordered in the triple mutant compared to the wild type. Although PIN1-GFP was localized on the side of the cells in the L1 layer facing the center of the predicted incipient flower primordia, no PIN1-GFP signal was detected in the inner side of the plasma membrane of the mutant meristem (Fig. 1*M,* Fig. S2). The same results for PIN1 localization were obtained by an immunolocalization analysis using a PIN1 antibody (Fig. S3).

Taken together, these data indicate that mutation of the *MAB4* family genes did not affect the pumping of auxin to the incipient organ primordium in the L1 layer, but did cause the loss of inward auxin transport from the L1 layer that acted as an auxin sink. Therefore, we suggest that *MAB4* family genes have a limited role in the control of PIN1 polarization during organ formation.

***MAB4* family genes are required for continued progression of flower development**

In the flank of the meristem, the cyclical changes in PIN1 expression and polarity correspond to the sites of incipient and young organ primordia (2, 4, 5). To determine whether phyllotactic patterning is maintained in the *mab4 mel1 mel2* meristem that lacks inward auxin flow, we performed three-dimentional (3D) confocal microscope imaging of PIN1-GFP expression in *mab4-2 mel1-1 mel2-1* inflorescence meristems. The 3D reconstructions confirmed the cyclic induction of PIN1-GFP expression that coincided with the initial formation of bulges (Fig. 2*A*). The locations of strong PIN1-GFP expression were spaced almost equidistantly in a spiral arrangement. Analysis of PIN1-GFP polarity in the mutant meristems by serial sectioning of the reconstructed 3D images (Fig. 2*B*) showed that PIN1-GFP polarity in the initiating bulges with strong GFP signals were oriented toward outer edge of the bulges. These results indicate that mutation of *MAB4* family genes had little apparent effect on initial flower development but prevented developmental progress in the organ primordia after initiation.

To confirm this conclusion, we analyzed expression of *LEAFY* (*LFY*), a late-stage marker of flower development (24), in *mab4-2 mel1-1 mel2-1* inflorescences. *LFY* specifies floral fate and is directly induced by the auxin-responsive transcription factor MP in the periphery of the reproductive meristem (25). We found that *pLFY::GUS* was strongly expressed around the wild-type inflorescence meristem (Fig. 2*C*). However, we could not detect GUS activity in *pLFY::GUS*-expressing *mab4 mel1 mel2* inflorescences (Fig. 2*D*). These results indicate that the restriction of auxin response to the L1 layer of the mutant meristem does not enable induction of *LFY* expression or the developmental progression of incipient flower primordia. Taken together, our data suggest that *MAB4* family genes promote flower development including floral fate specification through formation of an inward auxin flow from the

L1 layer to the inner cell layers, leading to internal auxin resposes in organ primordia.

_MP_ induces the expression of _MAB4_ family genes at the periphery of the inflorescence meristem

MAB4 family genes have overlapping but slightly different expression domains in organ primordia (10-13). The proteins they encode are polarized at the cell periphery and colocalize with PIN proteins at the plasma membrane (13). To investigate the functional domain of MAB4, MEL1, and MEL2 in inflorescences, we first conducted an immunolocalization analysis using a MAB4 antibody. As expected, the MAB4-specific signal was detected at the initiation site of organ primordia and strong expression was evident in the L1 layer and weak expression in inner cell layers; the positions of the signals colocalized with polarized PIN1 at the cell periphery (Fig. 3*A*-*C*). Next, we expressed functional MEL1-GFP and MEL2-GFP under the control of their own promoters and found that they were expressed at the flower initiation sites and were polarized in the same manner as MAB4 (Fig. S4). These data indicate that MAB4 family proteins in the initiation sites of organ primordia contribute to the change in auxin flow through the control of PIN1 localization.

Analysis of auxin behavior using *DR5rev::GFP* and PIN1-GFP markers suggested the possibility that the switch in auxin flow pattern might be induced by the auxin accumulated by active pumps (Fig. 1*C*-*I*). To determine whether *MAB4* family-dependent inward auxin flow is induced by auxin at the reproductive meristem, we performed an expression analysis of the *MAB4* family genes in response to auxin. As expected, treatment of the shoot apex with auxin increased the promoter activity of these genes in the meristem (Fig. S5). In addition, expression of the *MAB4* family genes was analyzed in the auxin-response deficient *mp* mutant. In the wild-type meristem, strong expression of *MAB4* family gene promoters was found in the initiation sites of

organ primordial (Fig. 3*D-F*); however, expression was severely reduced in pin-shaped inflorescences of *mp* mutants (Fig. 3*G-I*). The reduction in promoter activities was also found during embryogenesis (Fig. S6). Furthermore, *mp* mutation blocked auxin-induced up-regulation of the *MAB4* family gene expression in the meristem (Fig. S7). These results indicate that auxin could upregulate expression of the *MAB4* family genes via *MP* activity. The *MAB4* family genes have several auxin-responsive elements (AuxRE; TGTCTC/GAGACA) in their promoter regions to which auxin resnponse factors can bind (26, 27): there are five AuxREs in *MAB4*, two in *MEL1*, and one in *MEL2* (Fig. 3*J*). To investigate the contribution of AuxREs to their promoter activities in the inflorescence meristem, mutations were inserted into the AuxREs of the *MEL1* and *MEL2* promoters, as previous described (28) (Fig. 3*J*). Promoters with mutated AuxREs showed severely reduced activities (Fig. 3*K-N*). Thus, *MP* activates expression of *MAB4* family genes in the initiation sites of organ primordia by binding to the gene promoter sequences. Our findings suggest that *MP* is involved in the switch in auxin flow during flower development in addition to *MAB4* family genes. In pin-shaped inflorescences of the *mp-T370* mutant, PIN1 was strongly expressed in the L1 layer cells and was normally localized to the anticlinal side of the plasma membrane (Fig. 3*O-Q*). Convergence points of PIN1 polarity were normally found at the apex of the mutant meristem (Fig. 3*P* and *Q*). However, no obvious PIN1 signals were detected in the inner side of the plasma membrane in *mp* meristems, as well as in the *mab4 mel1 mel2* meristem (Fig. 3*P* and *Q*, Fig. S2). Although many of *mp* meristems displayed no signal of *DR5rev::GFP* (Fig. S8*A*), *DR5rev::GFP* was occasionally expressed over all the epidermis of *mp* meristem (Fig. S8*B*). These results indicate that *mp* causes the loss of inward auxin transport from the L1 layer as well as mutation in the *MAB4* family genes. Taken together, our observations suggest that *MP*-mediated auxin response establishes inward auxin transport through the up-regulation of *MAB4* family genes.

L1-specific *MAB4* induces auxin response in inner cell layers through a shift in PIN1 localization

Auxin response was previously shown to be restricted to the L1 layer prior to the switch in auxin flow (Fig. 1*C*); this suggests that the induction of *MAB4* family genes in response to auxin in the L1 layer is involved in the initiation of inward auxin transport at the sites of incipient organ primordia. To test this possibility, we expressed *MAB4* in an L1-specific manner in the *mab4 mel1 mel2* mutant background in which auxin accumulates in the L1 layer due to the failure of inward auxin transport. To identify changes in auxin flow, a plasmid expressing *MAB4* cDNA driven by the L1 specific promoter *pATML1* was transformed into *DR5rev::GFP* or PIN1-GFP expressing *mab4-2 mel1-1 mel2-1* triple mutants. We found that L1-specific *MAB4* expression almost completely rescued the *mab4 mel1 mel2* mutant phenotypes (Fig. 1*B* and 4*A*). The transgenic plants produced flower primordia and floral meristems around the inflorescence meristem with a phyllotactic pattern similar to that of the wild type (Fig. 4*E* and *G*), whereas the *mab4 mel1 mel2* triple mutant formed no flower meristems in the tip of the inflorescence (Fig. 4*F*). The L1-specific MAB4 expression in the transgenic plants was confirmed by an immunolocalization analysis using a MAB4 antibody (Fig. 4*H-J*). MAB4 was expressed not only in the L1 layer but also in the inner cell layers of flower primordia of wild-type plants, but not in *mab4-2 mel1-1 mel2-1* triple mutants (Fig. 4*H* and *I*). In the transformants, MAB4 was expressed specifically in the L1 layer, but not in inner cell layers (Fig. 4*J*). As expected, when MAB4 was expressed specifically in the surface of the *mab4 mel1 mel2* triple mutants, the expression of *DR5rev::GFP* expanded into the inner cell layers compared to that in the triple mutants (Fig. 1*J* and 4*B*). At the same time, *DR5rev::GFP* expression in the L1 layer narrowed to a small region around the meristem. Furthermore, L1-specific

expression of MAB4 localized PIN1-GFP to the inner side of the plasma membrane of L1 cells at the flower primordia initiation sites (Fig. 4*C* and *D*). These results indicate that MAB4 in the L1 layer alters auxin flow by inward PIN1 relocalization, resulting in an inward shift of auxin accumulation in the incipient organ primordia. This switch in auxin flow is sufficient for continued progression of flower development.

A Model for Auxin-Dependent Development of Flower Primordia

Our findings provide evidence for the existence of two distinct molecular pathways controlling PIN1 polarization in flower development and reveal a molecular framework for the switch between these two pathways. Mutation of three *MAB4* family genes specifically affects the basipetal PIN1 polarization, but not the convergence of PIN1 polarity in the L1 layer. This suggests that PIN1 convergence is at first MAB4-independet, but that subsequent basipetal PIN1 polarization is under the control of *MAB4* family genes. *PID* may function in the convergence of PIN1 polarity, because loss-of-function of *PID* results in basal PIN1 targeting and leads to failure to establish local auxin accumulation (20). PID (or other factors) may mediate the PIN1 convergence in the L1 layer that induces auxin accumulation at the initiation site of organ primordia (Fig. 4*K*). Auxin triggers the activation of the auxin-responsive transcription factor MP in the L1 layer. Auxin-activated MP then induces expression of *MAB4* family genes, which establishes inward auxin transport through basipetal PIN1 polarization in the L1 layer, possibly by affecting PID activity. Recently, NPH3, homologous to MAB4 family proteins, was reported to function as a substrate adapter in a CULLIN3-based E3 ubiquitin ligase for PHOTOTROPIN1 (PHOT1), which is a member of the same AGC kinase family as PID (29). Ubiquitination of PHOT1 modifies its activity through the control of the stability and localization of PHOT1 in phototropic response. The resulting accumulation of auxin in the inner cell regions also

up-regulates *MAB4* family gene expression via the activation of MP. Again, MAB4 family proteins localize PIN1 basally and promote inward auxin transport in the inner cells of the inflorescence meristems. This intercellular positive feedback mechanism enables consecutive PIN1 polarization and can explain the gradual establishment of inward auxin transport from the L1 layer. In this way, inward auxin flow provides sufficient auxin for inner cells to undergo cell proliferation, leading to organ outgrowth. Proper organ growth along the proximal-distal axis requires polarized cell proliferation and not random proliferation. When we fully complemented the triple mutant with L1-specific *MAB4* (Fig. 4), the auxin response in the distal region of the subepidermal cells sufficed for normal organ growth. Distally located cells might proliferate more rapidly than proximally located cells in response to auxin from the tip of the organ primordium. Currently, however, the function of *MAB4* family genes in subepidermal cells of organ primordia remains unknown. Interestingly, similar observation was recently reported. PIN1 expression in the L1 layer is sufficient for correct organ development with phyllotactic patterning (30). Further detailed analyses will provide biological insight into the roles of interlaminar connection in organ development. In summary, our study provides experimental proof for a theoretical model of aerial organ development and uncovers an unexpected mode of action of auxin based on a difference between the outermost and inner cell layers. The continued development of the organ primordium requires more than auxin on the surface, but rather needs an L1-to-inner cell layer auxin supply.

Materials and Methods

Plant materials and growth condition

Arabidopsis thaliana accession Columbia (Col) was used as the wild type. The following mutant alleles and transgenic plants were used: *mab4-2* (Col) (10), *mel1-1* (Col) and *mel2-1* (Col) (13), *mp-T370* (L*er*) (31), PIN1-GFP (Col) (32), *DR5rev::GFP* (Col) (20), *pLFY-GUS* (Col) (24), *pMEL1-MEL1-GFP* (Col), *pMEL2-MEL2-GFP* (Col), *pMAB4-GUS* (Col), *pMEL1-GUS* (Col), and *pMEL2-GUS* (Col) (13). Plants were grown on soil as previously described (33).

Transgenic plants

To construct the plasmid *pMEL1(aB)-GUS*, *pMEL1(Ab)-GUS*, *pMEL1(ab)-GUS*, and *pMEL2(a)-GUS*, point mutations were introduced into the AuxREs of the *MEL1* and *MEL2* promoters by PCR amplification of the plasmids containing wild-type promoters The following primer pairs were used: pMEL1-mA-fw (5'-GATTTTCACAGTGTTGGCTCCTTAAG-3') and pMEL1-mA-rv (5'-CTTAAGGAGCCAACACTGTGAAAATC-3'). pMEL1-mB-fw (5'-TAGTGGTGTTGGCTCATGATTAAG-3') and pMEL1-mB-rv (5'-CTTAATCATGAGCCAACACCACTA-3'). pMEL2-mA-fw (5'-ATTCTTCGATTGAGCCAAATCCTGGGTTAT-3') and pMEL2-mA-rv (5'-ATAACCCAGGATTTGGCTCAATCGAAGAAT-3'). In the construction of *pMEL(ab)-GUS*, PCR amplification was performed from the mutated *MEL1* promoter, *pMEL1(aB)*, using the primers pMEL1-mB-fw and pMEL1-mB-rv. After PCR amplification, the templates were digested with Dpn I. Then, the mutated promoters were inserted upstream of the GUS gene in the binary vector pBI101. For *pATML1-MAB4*, *MAB4* cDNA was cloned using PCR and inserted under the *ATML1* promoter in the plasmid *pATML::NOSt* in the pGreen II vector (34). Then,

pATML-MAB4::NOSt was transferred into the pBIN50 vector. These plasmids were introduced into Col using *Agrobacterium tumefaciens* strain MP90. *pMEL1(aB)-GUS*, *pMEL1(Ab)-GUS*, *pMEL1(ab)-GUS*, and *pMEL2(a)-GUS* vectors were transformed into Col by the floral dip method (35). *pATML1-MAB4* was transformed into heterozygous *mab4-2* and *mel1-1*, and homozygous *mel2-1* plants expressing *DR5rev::GFP* or PIN1-GFP. For *pMEL1(aB)-GUS*, *pMEL1(Ab)-GUS*, *pMEL1(ab)-GUS*, and *pMEL2(a)-GUS*, transformants were selected on germination medium containing 30 μg/ml kanamycin; for *pATML1-MAB4*, selection was performed using 20 μg/ml hygromycin. Homozygous lines were identified in the T3 generation, and T3 or T4 homozygous lines were used for the reporter analysis.

Microscopy

Confocal laser-scanning microscopy (FV1000; Olympus) was carried out on inflorescence meristems mounted in MS liquid medium (1/2 MS salt mixture and 1 % sucrose). Confocal microscopy based 3D imaging was carried out using pin-shaped inflorescence meristems mounted in 1 % agarose medium. The 3D reconstructions were performed using ImageJ to adjust the z-axis. Then, reconstructed inflorescences were sectioned transversely at 10 μm intervals using ImageJ.

GUS staining

To detect GUS activity, tissues were fixed in chilled 90 % acetone for 15 minutes and washed briefly twice with 100 mM phosphate buffer. Fixed tissues were stained at 37 °C in the dark with the solution described previously (36). Stained tissues were dehydrated in a graded ethanol series (30, 50, 70, 90 and 100 %) for 15 minutes and then rehydrated in a graded ethanol series (90, 70, 50 and 30 %) for 15 minutes. Tissues were cleared as previously described (37) and analyzed using an Eclipse E800

Nomarski microscope (Nikon).

Immunolocalization

Immunofluorescence analysis of sections of inflorescence meristems was performed as described previously (2). Antibodies were diluted as follows: 1:500 for rabbit anti-MAB4, 1:200 for goat anti-PIN1 (Santa Cruz Biotechnology), 1:500 for Alexa488- and Alexa647-conjugated anti-goat and rabbit secondary antibodies (Invitrogen), respectively.

References

1. Reinhardt D, Mandel T, Kuhlemeier C (2000) Auxin regulates the initiation and radial position of plant lateral organs. *Plant Cell* 12: 507-518.

2. Reinhardt D, et al. (2003) Regulation of phyllotaxis by polar auxin transport. *Nature* 426: 255-260.

3. Benková E, et al. (2003) Local, efflux-dependent auxin gradients as a common module for plant organ formation. *Cell* 115: 591-602.

4. Heisler MG, et al. (2005) Patterns of auxin transport and gene expression during primordium development revealed by live imaging of the *Arabidopsis* inflorescence meristem. *Curr Biol* 15: 1899-1911.

5. Bayer EM, et al. (2009) Integration of transport-based models for phyllotaxis and midvein formation. *Genes Dev* 23: 373-384.

6. Mitchison GJ (1980) Model for vein formation in higher-plants. *Proc R Soc Lond B Biol Sci* 207: 79-109.

7. Jönsson H, et al. (2006) An auxin-driven polarized transport model for phyllotaxis. *Proc Natl Acad Sci USA* 103: 1633-1638.

8. Smith RS, et al. (2006) A plausible model of phyllotaxis. *Proc Natl Acad Sci USA* 103: 1301-1306.

9. de Reuille PB, et al. (2006) Computer simulations reveal properties of the cell-cell signaling network at the shoot apex in *Arabidopsis*. *Proc Natl Acad Sci USA* 103: 1627-1632.

10. Furutani M, et al. (2007) The gene *MACCHI-BOU 4*/*ENHANCER OF PINOID* encodes a NPH3-like protein and reveals similarities between organogenesis and phototropism at the molecular level. *Development* 134: 3849-3859.

11. Cheng Y, Qin G, Dai X, Zhao Y (2007) NPY1, a BTB-NPH3-like protein, plays a critical role in auxin-regulated organogenesis in *Arabidopsis*. *Proc Natl Acad Sci USA* 104: 18825-18829.

12. Cheng Y, Qin G, Dai X, Zhao Y (2008) *NPY* genes and AGC kinases define two key steps in auxin-mediated organogenesis in *Arabidopsis*. *Proc Natl Acad Sci USA* 105: 21017-21022.

13. Furutani M, et al. (2011) Polar-localized NPH3-like proteins regulate polarity and endocytosis of PIN-FORMED auxin efflux carriers. *Development* 138: 2069-2078.

14. Okada K, et al. (1991) Requirement of the Auxin Polar Transport System in Early Stages of Arabidopsis Floral Bud Formation. *Plant Cell* 3: 677-684.

15. Bennett SRM, Alvarez J, Bossinger G, Smyth DR (1995) Morphogenesis in *pinoid* mutants of *Arabidopsis thaliana*. *Plant J* 8: 505-520.

16. Przemeck GK, et al. (1996) Studies on the role of the *Arabidopsis* gene *MONOPTEROS* in vascular development and plant cell axialization. *Planta* 200: 229-237.

17. Christensen SK, Dagenais N, Chory J, Weigel D (2000) Regulation of auxin response by the protein kinase PINOID. *Cell* 100: 469-478.

18. Benjamins R, et al. (2001) The PINOID protein kinase regulates organ development in *Arabidopsis* by enhancing polar auxin transport. *Development* 128: 4057-4067.

19. Michniewicz M, et al. (2007) Antagonistic regulation of PIN phosphorylation by PP2A and PINOID directs auxin flux. *Cell* 130: 1044-1056.

20. Friml J, et al. (2004) A PINOID-dependent binary switch in apical-basal PIN polar targeting directs auxin efflux. *Science* 306: 862-865.

21. Hardtke CS, Berleth T (1998) The *Arabidopsis* gene *MONOPTEROS* encodes a transcription factor mediating embryo axis formation and vascular development. *Embo j* 17: 1405-1411.

22. Treml BS, et al (2005) The gene *ENHANCER OF PINOID* controls cotyledon development in the *Arabidopsis* embryo. *Development* 132: 4063-4074.

23. Friml J, et al. (2003) Efflux-dependent auxin gradients establish the apical-basal axis of *Arabidopsis*. *Nature* 426: 147-153.

24. Blázquez MA, Soowal LN, Lee I, Weigel D (1997) *LEAFY* expression and flower initiation in *Arabidopsis*. *Development* 124: 3835-3844.

25. Yamaguchi N, et al. (2013) A molecular framework for auxin-mediated initiation of flower primordia. *Dev Cell* 24: 271-282.

26. Ballas N, Wong LM, Theologis A (1993) Identification of the auxin-responsive element, AuxRE, in the primary indoleacetic acid-inducible gene, PS-IAA4/5, of pea (Pisum sativum). *J Mol Biol* 233: 580-596.

27. Ulmasov T, Hagen G, Guilfoyle TJ (1999) Activation and repression of transcription by auxin-response factors. *Proc Natl Acad Sci USA* 96: 5844-5849.

28. Ulmasov T, Hagen G, Guilfoyle TJ (1997) ARF1, a trascription factor that binds to auxi response elements. *Science* 276: 1865-1868

29. Roberts D, et al. (2011) Modulation of phototropic responsiveness in *Arabidopsis* through ubiquitination of phototropin 1 by the CUL3-Ring E3 ubiquitin ligase $CRL3^{NPH3}$. *Plant Cell* 23: 3627-3640.

30. Kierzkowski D, Lenhard M, Smith R, Kuhlemeier C. (2013) Interaction between meristem tissue layers controls phyllotaxis. *Dev Cell* 26: 616-628.

31. Weijers D, et al. (2006) Auxin triggers transient local signaling for cell specification in *Arabidopsis* embryogenesis. *Dev Cell* 10: 265-270.

32. Xu J, et al. (2006) A molecular framework for plant regeneration. *Science* 311: 385-388.

33. Fukaki H, Fujisawa H, Tasaka M (1996) Gravitropic response of inflorescence stems in *Arabidopsis thaliana*. *Plant Physiol* 110: 933-943.

34. Takada S, Jürgens G (2007) Transcriptional regulation of epidermal cell fate in the *Arabidopsis* embryo. *Development* 134: 1141-1150.

35. Clough S, Bent A (1998) Floral dip: a simplified method for *Agrobacterium*-mediated transformation of *Arabidopsis thaliana*. *Plant J* 16: 735-743.

36. Takada S, Hibara K, Ishida T, Tasaka M (2001) The *CUP-SHAPED*

COTYLEDON1 gene of *Arabidopsis* regulates shoot apical meristem formation. *Development* 128: 1127-1135.

37. Aida M, et al. (1997) Genes involved in organ separation in Arabidopsis: an analysis of the *cup-shaped cotyledon* mutant. *Plant Cell* 9: 841-857.

Acknowledgements

We thank Ben Scheres and Jiří Friml for providing us with PIN1-GFP and *DR5rev::GFP* expressing plants, and Shinobu Takada for providing the plasmid pATML1::NOSt/pGreen II KAN #8. We also would like to thank Asami Mori for excellent technical assistance, Cris Kuhlemeier, Jun Ito, and Norihito Sakamoto for their suggestions and critical reading of our manuscript. This work was partly supported by the Ministry of Education, Culture, Sports, Science and Technology, through Grants in Aid for Scientific Research on Priority Areas (14036222 and 19060007) to M.T., Grant-in-Aid for Young Scientists (20770034) and Global COE Program in NAIST (Frontier Biosciences: strategies for survival and adaptation in a changing global enviroment), MEXT, Japan to M.F.

Figure Legends

Fig. 1. *MAB4* family genes control polar auxin transport in the inflorescence meristem

(*A* and *B*) Inflorescences of wild type (*A*) and *mab4-2 mel1-1 mel2-1* triple mutants (*B*). (*C-F*) *DR5rev::GFP* expression in wild-type inflorescence meristems. GFP fluorescence images (*left*) and merged images with Nomarski images (*right*). Arrowheads in d-f indicate the GFP signal in inner cells. Asterisks represent inflorescence meristems. I1, immature floral primordium; P1, P2, P3 indicate the stage of floral primordia. (*G-I*) PIN1-GFP expression in wild-type inflorescences. GFP fluorescence images (*top*) and merged images with Nomarski images (*bottom*). Arrows in (*G-I*) demonstrate the predicted polar auxin transport at the organ initiation site. White arrows indicate pumping-up auxin transport, while orange ones do basipetal auxin transport. Arrowheads in H and I indicate PIN1-GFP localization in the inner side of the plasma membrane. (*J* and *L*) *DR5rev::GFP* (*J*) and PIN1-GFP (*L*) expression in *mab4-2 mel1-1 mel2-1* inflorescence meristems. GFP fluorescence images (*left*) and merged images with Nomarski images (*right*). Asterisks indicate inflorescence meristems. (*K* and *M*) Magnified images of the peripheral region of the triple mutant meristem in (*J*) and (*L*), respectively. The asterisk in (*M*) indicates a convergence point of PIN1-GFP polarity. Scale bars represent 20 μm.

Fig. 2. Flower development in *mab4 mel1 mel2* triple mutants

(*A*) 3D image of PIN1-GFP expression in the *mab4-2 mel1-1 mel2-1* inflorescence meristem. Predicted flower primordia were numbered from the youngest I to the older. (*B*) Serial transverse sections of PIN1-GFP in the *mab4-2 mel1-1 mel2-1* meristem. Interval scale is 10 μm. Arabic numerals indicate the order of slice counted from the top of the meristem. Roman numbers represent the order of initiation of predicted flower

primordia, numbered from the youngest I. No convergence of PIN1-GFP occurred with low frequency in spite of relatively strong expression and bulging (I'). (*C* and *D*) *pLFY::GUS* activity. GUS staining was detected in the wild-type flower meristems (*C*), but not in the pin-shaped inflorescence of the *mab4-2 mel1-1 mel2-1* mutant (*D*). Scale bars represent 10 µm (*A* and *B*) and 100 µm (*C* and *D*).

Fig. 3. *MAB4* family genes are up-regulated by auxin responsive MP

(*A-C*) Immunolocalization of MAB4 (*A*) and PIN1 (*B*) in the inflorescence meristem. Merged image showing MAB4 (*red*) and PIN1 (*green*) staining in the meristem (*C*). (*D-I*) GUS staining of *pMAB4::GUS* (*D* and *G*), *pMEL1::GUS* (*E* and *H*), and *pMEL2::GUS* (*F* and *I*) in the inflorescence meristem of the wild type (*D-F*) and *mp-T370* (*G-I*). Asterisks indicate inflorescence meristems. Arrowheads in (*D-F*) indicate the initiation sites of flower primordia. (*J*) Position of AuxREs in the promoter regions of *MEL1* (*left*) and *MEL2* (*right*). Standard AuxREs are indicated by capital letters (A, B; orange box) and mutated AuxREs are indicated by lowercase letters (a, b; gray box). (*K-N*) GUS staining of mutated *pMEL1::GUS* (*K-M*) and *pMEL2::GUS* (*N*) in wild-type inflorescences. Asterisks indicate inflorescence meristems. Arrowheads indicate the initiation sites of flower primordia. (*O*) Inflorescences of the *mp-T370* mutant. Arrows point to pin-shaped inflorescences. (*P* and *Q*) Immunolocalization of PIN1 (*P*) and PIN1-GFP expression (*Q*) in the *mp-T370* inflorescence. Arrows indicate the predicted polar auxin transport at the peripheral region of the mutant meristem. White arrows indicate pumping-up auxin transport, while orange ones show basipetal auxin transport. The asterisk indicates a convergence point of PIN1 and PIN1-GFP polarity. Scale bars represent 20 µm.

Fig. 4. L1-specific *MAB4* dissipates the accumulated auxin in the *mab4-2 mel1-1*

***mel2-1* inflorescence meristem**

(*A*) Inflorescence of a *pATML1::MAB4* / *mab4-2 mel1-1 mel2-1* plant. (*B-D*) GFP fluorescent images of *DR5rev::GFP* (*B*) and PIN1-GFP (*C* and *D*) in the *pATML1::MAB4* / *mab4-2 mel1-1 mel2-1* inflorescence meristems. Asterisks indicate inflorescence meristems. Arrows in B represent the narrow region of *DR5rev::GFP* expression in the L1 layer and arrowheads in B indicate *DR5rev::GFP* expression in the inner cell layer of the inflorescence meristem. (*D*) A magnified image of the flower primordium shown in (*C*). Arrowheads in (*D*) indicate PIN1-GFP localization in the inner side of the plasma membrane. (*E-G*) Scanning electron micrographs of wild type (*E*), *mab4-2 mel1-1 mel2-1* (*F*), and *pATML1::MAB4* / *mab4-2 mel1-1 mel2-1* inflorescences (*G*). (*H-J*) MAB4 localization in wild type (*H*), *mab4-2 mel1-1 mel2-1* (*I*), and *pATML1::MAB4* / *mab4-2 mel1-1 mel2-1* inflorescences (*J*). Arrowheads in (*H*) indicate MAB4 signals in the inner cell layer of the wild-type inflorescence meristem. (*K*) A model for the two distinct mechanisms of auxin transport: convergent PIN1 polarization (*left*) and basipetal PIN1 polarization (*right*). Scar bars represent 20 μm (*B-D* and *H-J*) and 100 μm (*E-G*).

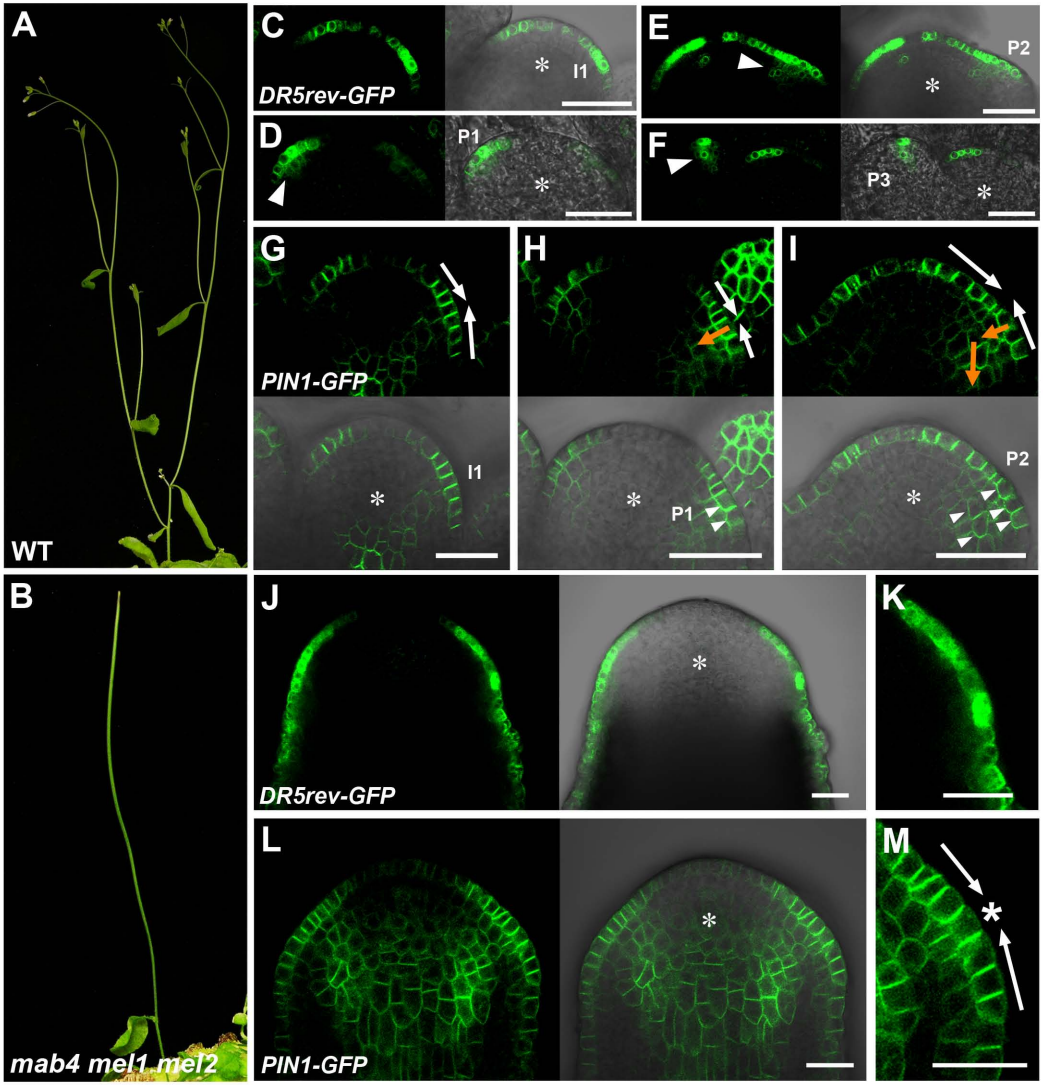
A
WT
B
mab4 mel1 mel2
C
DR5rev-GFP
I1
D
P1
E
P2
F
P3
G
PIN1-GFP
I1
H
P1
I
P2
J
DR5rev-GFP
K
L
PIN1-GFP
M

Figure 1

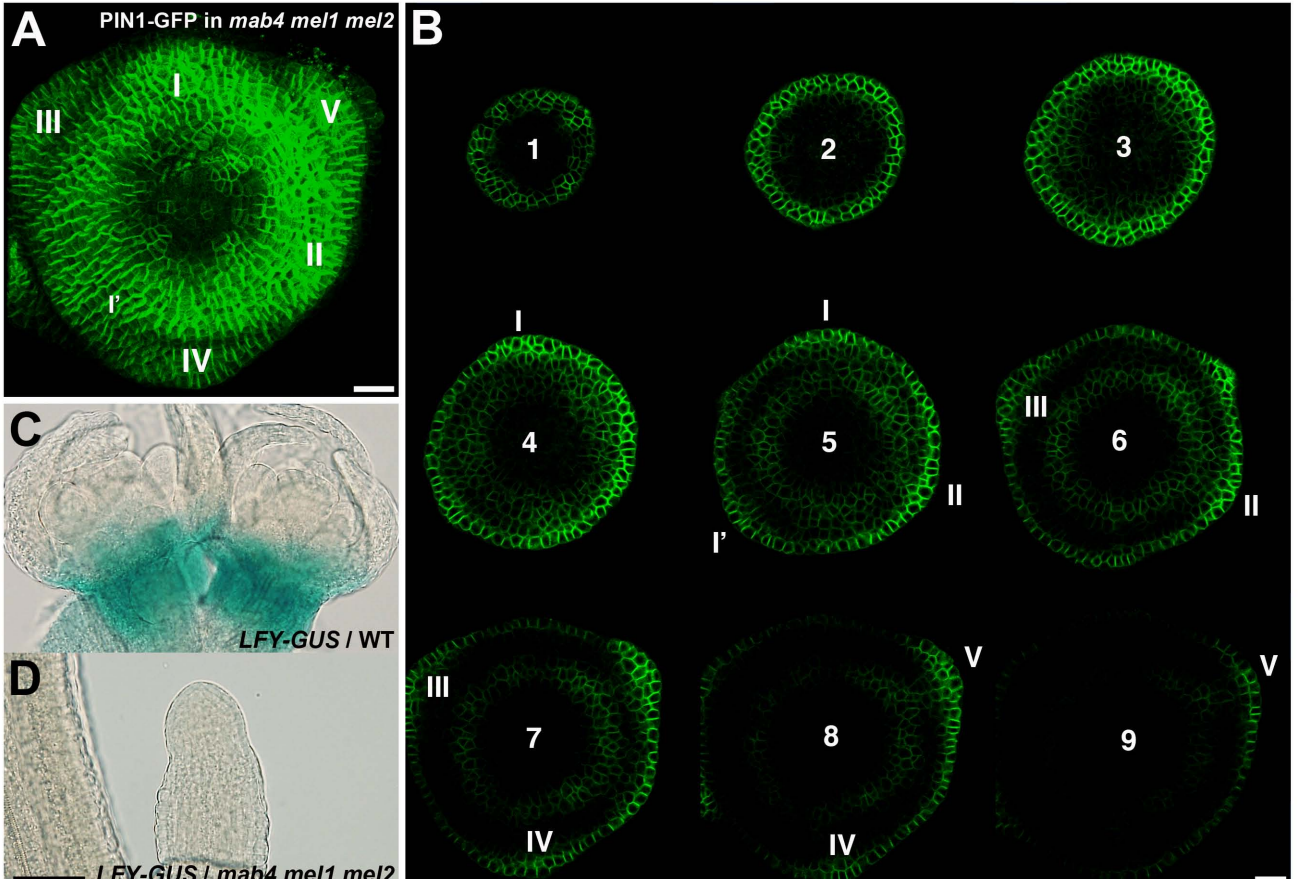
A
PIN1-GFP in mab4 mel1 mel2
I
V
III
II
I'
IV
B
1
2
3
I
4
I
5
II
I'
III
6
II
III
7
IV
V
8
IV
V
9
C
LFY-GUS / WT
D
LFY-GUS / mab4 mel1 mel2

Figure 2

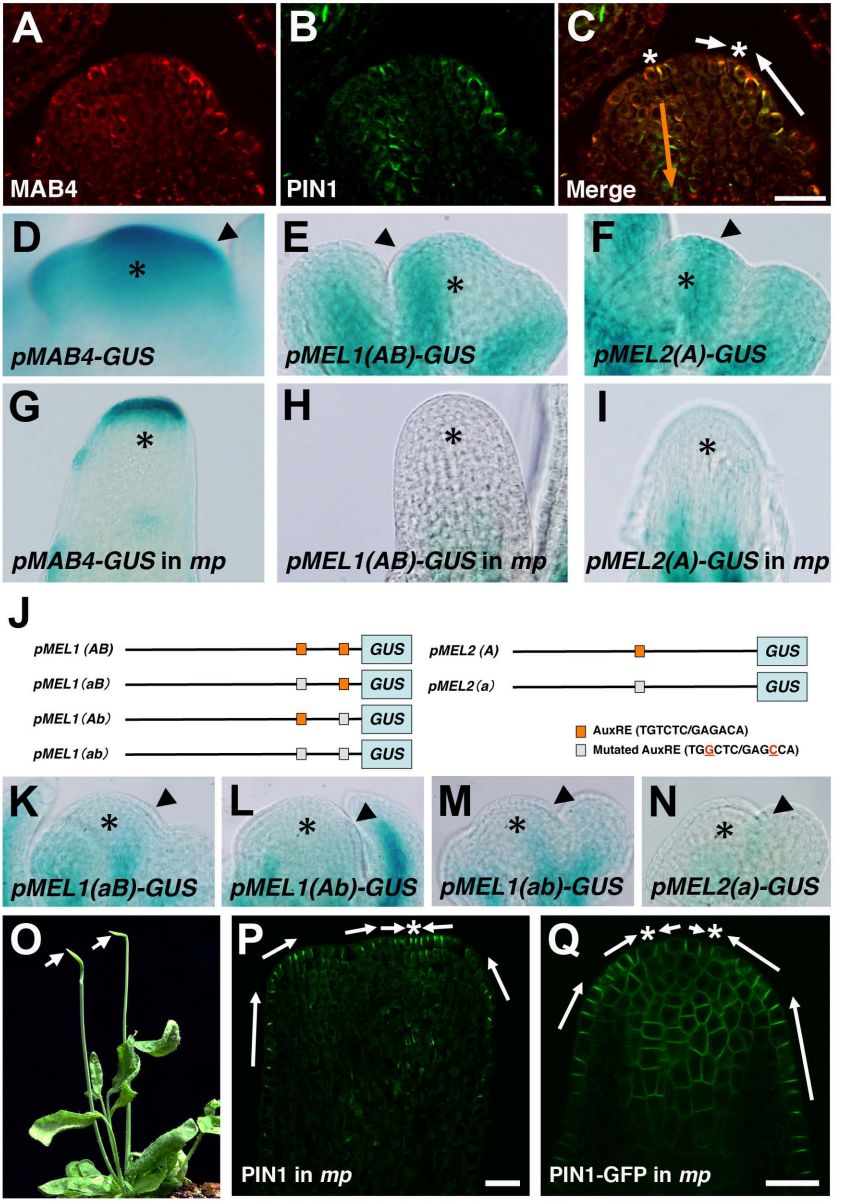
A
MAB4
B
PIN1
C
Merge
D
pMAB4-GUS
E
pMEL1(AB)-GUS
F
pMEL2(A)-GUS
G
pMAB4-GUS in mp
H
pMEL1(AB)-GUS in mp
I
pMEL2(A)-GUS in mp
J
pMEL1 (AB)
pMEL1 (aB)
pMEL1 (Ab)
pMEL1 (ab)
pMEL2 (A)
pMEL2 (a)
GUS
AuxRE (TGTCTC/GAGACA)
Mutated AuxRE (TGGCTC/GAGCCA)
K
pMEL1(aB)-GUS
L
pMEL1(Ab)-GUS
M
pMEL1(ab)-GUS
N
pMEL2(a)-GUS
O
P
PIN1 in mp
Q
PIN1-GFP in mp

Figure 3

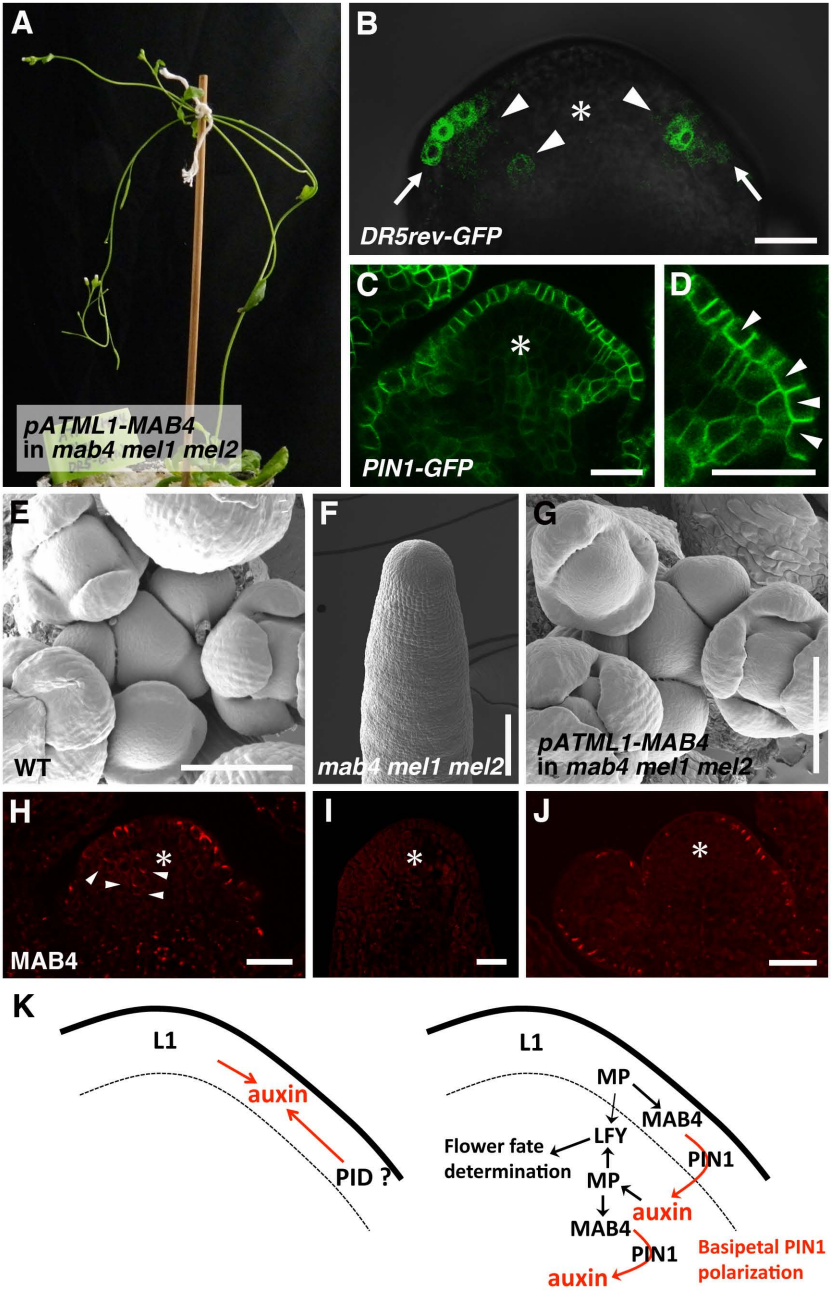
A
pATML1-MAB4
in mab4 mel1 mel2
B
DR5rev-GFP
C
PIN1-GFP
D
E
WT
F
mab4 mel1 mel2
G
pATML1-MAB4
in mab4 mel1 mel2
H
MAB4
I
J
K
L1
auxin
PID ?
L1
MP
MAB4
Flower fate
determination
LFY
PIN1
MP
auxin
MAB4
PIN1
Basipetal PIN1
polarization
auxin

Figure 4

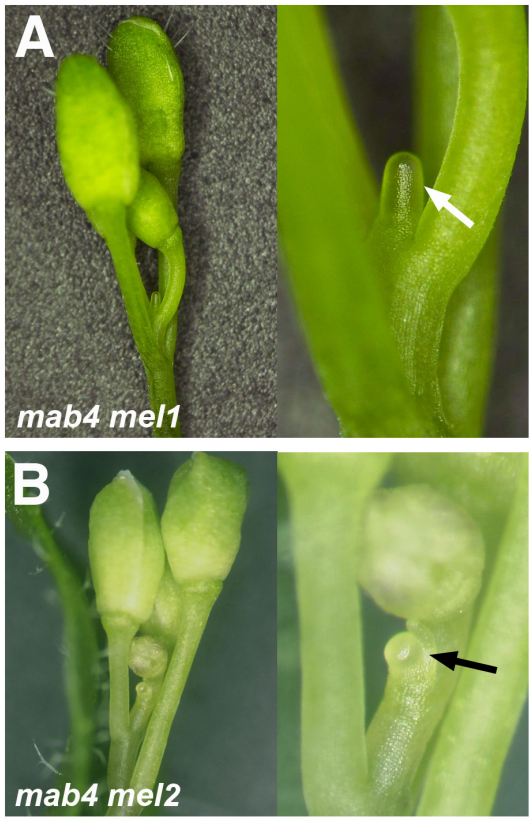

Fig. S1. Mutation of *mel1* and *mel2* enhances the *mab4* phenotypes.

(*A* and *B*) Inflorescences of *mab4-2 mel1-1* (*A*) and *mab4-2 mel2-1* double mutants (*B*). The right panel of (*A*) and (*B*) shows a magnified image around the inflorescence meristem, respectively. Arrows indicate pin-shaped inflorescences.

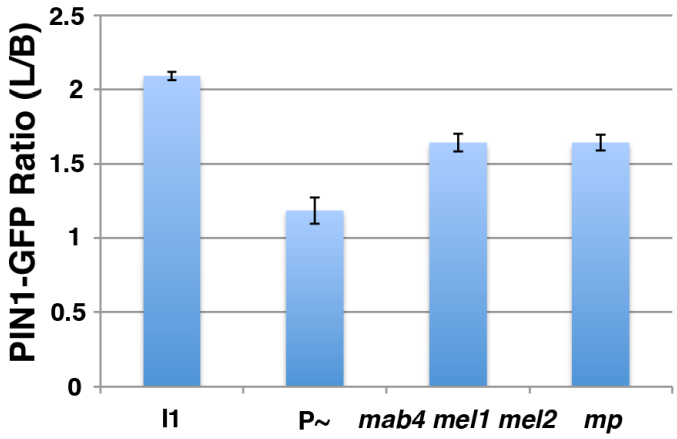

Fig. S2. The ratio of PIN1-GFP intensity on lateral side to that on bottom side of plasma membrane of epidermis.

The graph displays the ratio of intensity of PIN1-GFP fluorescence on lateral side to that on bottom side of epidermis around the convergence points of PIN1-GFP in wild-type immature primordia (I1) and developing primordia (P~), *mab4-2 mel1-1 mel2-1*, and *mp-T370* [N_{I1}=14, $N_{P\sim}$=12, $N_{mab4\ mel1\ mel2}$=12, N_{mp}=12]. Error bars represent s.e.m.

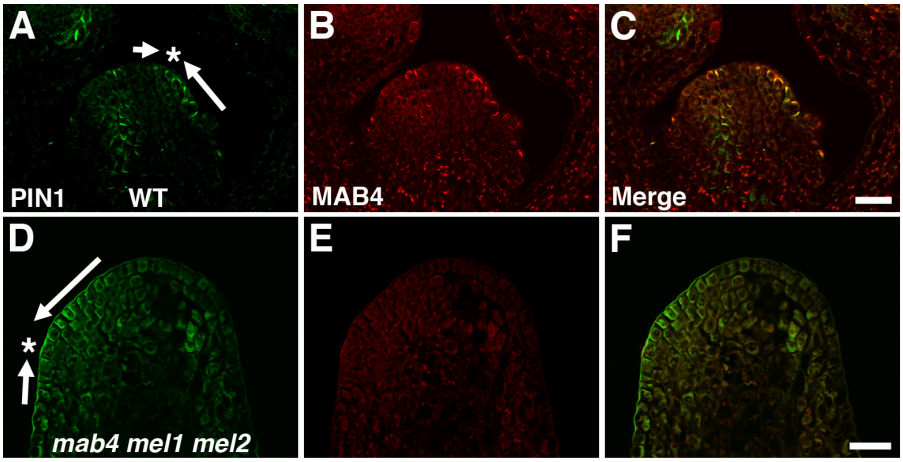

Fig. S3. PIN1 and MAB4 localization in *mab4-2 mel1-1 mel2-1* triple mutants.

(*A*-*C*) Immunolocalization of PIN1 (*A*) and MAB4 (*B*) in the wild-type inflorescence meristem. Cells co-labeled with PIN1 (*green*) and MAB4 (*red*) are seen as yellow signals in the merged image (*C*). Arrows indicate predicted polar auxin transport. The asterisk indicates a convergence point of PIN1 polarity. (*D*-*F*) PIN1 (*D*) and MAB4 (*E*) localization in a *mab4-2 mel1-1 mel2-1* inflorescence. Merged image of PIN1 (*green*) and MAB4 (*red*) staining (*F*). Scale bars represent 20 μm.

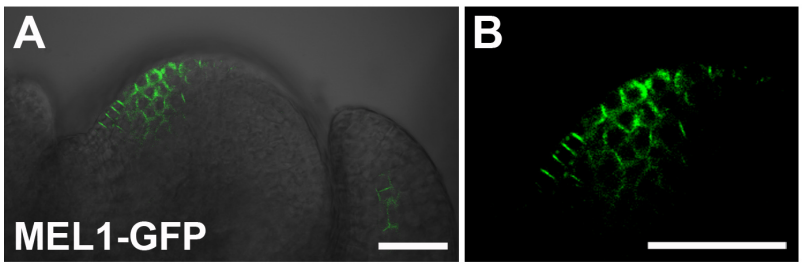

Fig. S4. MEL1-GFP localization in the inflorescence meristem.

(*A* and *B*) GFP fluorescence images of MEL1-GFP, merged with the Nomarski image (*A*) and magnified at the peripheral region of the meristem (*B*). Scale bars represent 20 μm.

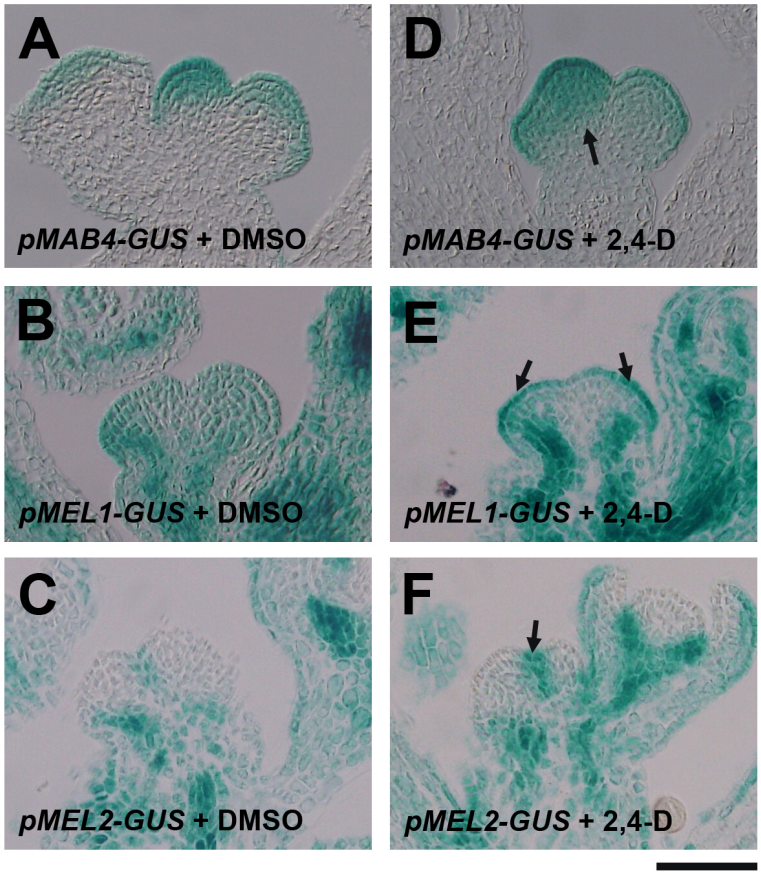

Fig. S5. Auxin treatment upregulated expression of the *MAB4* family genes.

(*A-F*) GUS staining of *pMAB4::GUS* (*A* and *D*), *pMEL1::GUS* (*B* and *E*), and *pMEL2::GUS* (*C* and *F*) in inflorescences, treated with DMSO (*A-C*) and 10μM 2,4-D (*D-F*) for 6 hours, respectively. Arrows in *D-F* show increased GUS staining. Scale bar for *A-F* represents 100 μm.

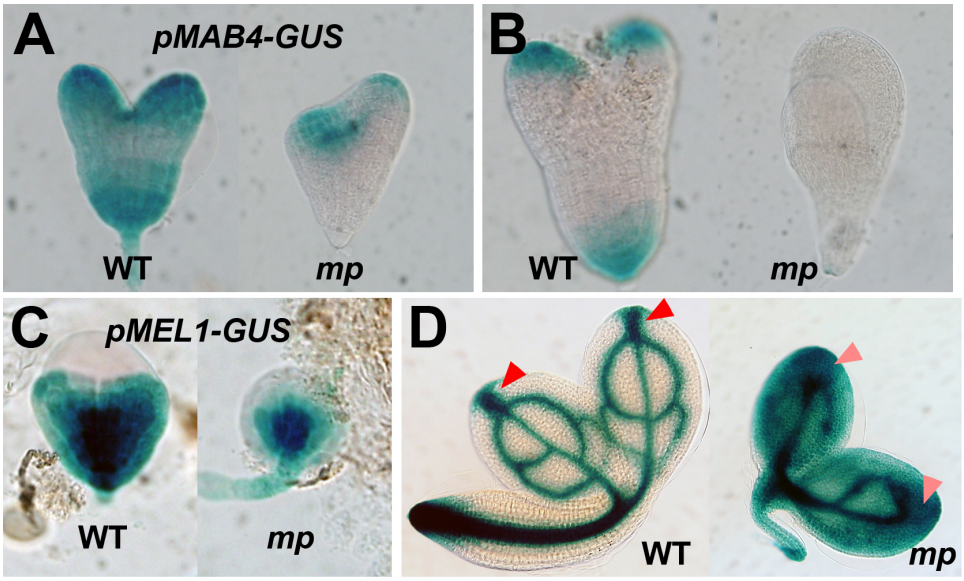

Fig. S6. Decreased expression of the *MAB4* family genes during embryogenesis.

(*A* and *B*) GUS staining of *pMAB4::GUS* in the wild-type (*left*) and *mp-T370* (*right*) embryos at the heart (*A*) and torpedo stage (*B*). (*C* and *D*) GUS staining of *pMEL1::GUS* in the wild-type (*left*) and *mp-T370* (*right*) embryos at the heart (*C*) and mature stage (*D*). Red arrowheads in (*D*) indicate GUS activity at the tips of cotyledon. Strong GUS staining was detected in wild type (*left*), but reduced GUS staining was found in *mp-T370* (*right*).

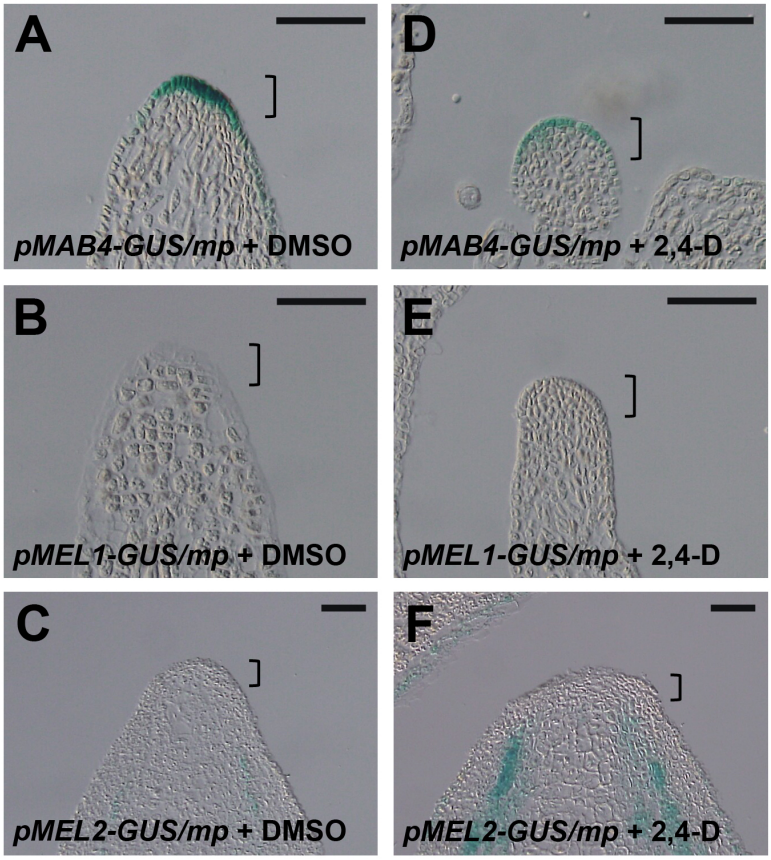

Fig. S7. No effect of auxin treatment on the *MAB4* family gene expression in *mp* inflorescences.

(*A-F*) GUS staining of *pMAB4::GUS* (*A* and *D*), *pMEL1::GUS* (*B* and *E*), and *pMEL2::GUS* (*C* and *F*) in *mp-T370* inflorescences, treated with DMSO (*A-C*) and 10μM 2,4-D (*D-F*) for 6 hours, respectively. Brackets in *A-F* show meristem area. Scale bars represent 100 μm.

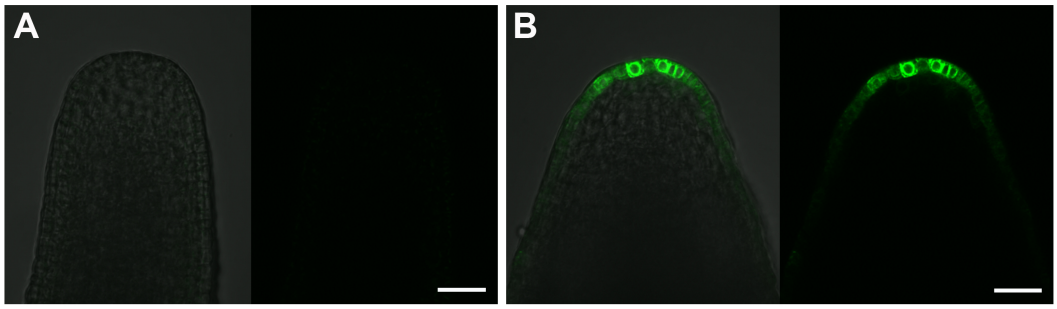

Fig. S8. *DR5rev::GFP* expression in *mp* inflorescences.

(*A* and *B*) *DR5rev::GFP* expression in pin-shaped inflorescences of *mp-T370*. GFP fluorescence images (*right*) and merged images with Nomarski images (*left*). Many of mutant meristem displayed no GFP signal (A). GFP signal was occasionally found in the L1 layer of the mutant apex (B). Scale bars represent 20 μm.